Tethered Satellite Retrieval with Thruster Augmented Control

Arun K. Banerjee*
Lockheed Missiles & Space Company, Inc., Sunnyvale, California
and
Thomas R. Kane†
Stanford University, Stanford, California

Retrieval of a Shuttle-based tethered satellite is examined. A reel torque control law is synthesized by drawing on the work of previous investigators, and it is shown that such control, alone, may be insufficient to prevent tether slackness and/or angle buildup. Therefore it is recommended that thrusters be employed for control augmentation. Specifically, it is shown that objectionable transverse motions can be attenuated by means of side-thrusters, while slackness can be prevented by employing tether-aligned thrusters. Simulations based on a dynamic model providing for an extensible, massive, straight-line tether in a central gravity field and subject to atmospheric drag are performed to demonstrate that use of the postulated control law leads to significant reductions in retrieval time.

I. Introduction

DYNAMICS and control of an Orbiter-based tethered satellite have been subjects of a number of detailed studies in recent years.[1-9] As a result, it has become known that of the three operations one must perform with such a satellite, namely, deployment, stationkeeping, and retrieval, the last is by far the most difficult, for the retrieval process is inherently unstable. This issue has been confronted in Refs. 1, 5-7, and 9, all of which involve the concept of "tension control," introduced by Rupp,[5] the underlying procedure being to vary tether tension as a specified function of commanded length, instantaneous length, and the time-derivative of this length. Significant additions to Rupp's tension control law subsequently were made by Bainum and Kumar,[7] who used optimal regulator theory to derive control gains; by Kulla,[6] who introduced out-of-plane angle rate-feedback; and by Modi et al.,[9] who demonstrated beneficial effects of employing feedback of both in-plane and out-of-plane angles and their time-derivatives.

In Refs. 4 and 8, both tether extensibility and flexibility are taken into account. When this is done, simulations tend to become very expensive for relatively short tethers. Indeed, it appears that the cost of simulating motions of a tether less than 5 km long is prohibitive, which means that information of crucial importance in connection with the terminal stage of the retrieval process cannot be obtained from such a model. With this in mind, and believing that extensibility is more important than flexure, especially for short tether lengths, we exclude flexure throughout what follows, hoping thus to produce a model that makes up in usefulness as a control law design tool what it lacks in modeling fidelity. The approach employed to model tether extensibility, which is the same as that in Ref. 10, leads to an algorithm that permits one to simulate complete retrievals at a very low computational cost.

Returning to the question of control strategy, we note that tension control, while appealingly simple, has the serious drawback that it is inherently unreliable during the terminal stage of a retrieval process because tether tension then becomes very small, vanishing totally when the satellite reaches the Orbiter. For example, in the case of a 450-kg satellite, such as the one being considered in connection with future Shuttle flights, the tension falls below 2 N when the satellite comes within 1 km of the Shuttle. Moreover, even this small tension is subject to reduction due to longitudinal tether oscillations possible in a real, and hence extensible, tether. In fact, it can be shown by means of simulations based on a model allowing extensibility that the tether must be expected to become slack long before the satellite comes into the vicinity of the Orbiter, unless retrieval is extremely slow, requiring, say, more than 25 h in the case of a 100-km-long tether. To overcome this difficulty, we propose that natural tether tension be augmented with a satellite-based, tether-aligned thruster, and that thrusters capable of exerting forces transverse to the tether be employed to stabilize and speed up the retrieval process. Other authors may have deliberately avoided the use of thrusters. It is the purpose of this paper to demonstrate the necessity and benefit of using thruster control in conjunction with tension control.

The sequel is divided into three parts. In Sec. II, simulation results are used to make a detailed comparison between two retrievals, one effected in the usual way, that is, with tension control alone, and the other involving tension control together with thrust augmentation of tension and transverse thrust control. In addition, it is shown that retrieval time can be reduced substantially through proper use of thrusters. The theoretical basis for these results is set forth in Sec. III, and some concluding remarks appear in Sec. IV.

II. Effects of Thrust Augmentation

A given retrieval process is characterized here by four functions of time, namely, tether tension, length, in-plane angle, and out-of-plane angle. (The latter two are defined with precision in Sec. III.) Therefore, to compare two retrievals, we present four plots (Figs. 1-4), each plot containing two curves, the dashed one corresponding to retrieval with tension control alone, whereas the solid one reveals the effects of using both tension and thrust control.

All of these results are presented with the "worst case" idea in mind; that is, the Shuttle is assumed to be in an Earth polar orbit, which gives rise to the most severe aerodynamic excitation. The values of initial in-plane and out-of-plane angles, -0.1 and 0.1 rad, respectively, are considerably greater than their normal steady-state values at the end of stationkeeping, namely, -0.05 and 0.004 rad, respectively. Let us examine Figs. 1-4 one at a time.

Received July 9, 1982; presented as Paper 82-1421 at the AIAA Guidance and Control, Atmospheric Flight Mechanics, and Astrodynamics Conference, San Diego, Calif., Aug. 9-11, 1982; revision received April 1, 1983.

*Research Specialist, Organization 62-61, Space Systems Division.
†Professor, Department of Mechanical Engineering.

The two curves in Fig. 1 are indistinguishable from each other for the first few hours of the retrival, but an important difference becomes apparent thereafter: The dashed curve crosses the horizontal axis at $t = 6.65$ h, indicating that the tether becomes slack at this instant, whereas the solid curve remains above the t axis at all times. No dashed curve is continued beyond $t = 6.75$ h in Figs. 1-4, as a retrieval cannot be continued with a slack tether.

In Fig. 2, the solid curve reveals that a rather smooth retrieval, from 100 km to 9 m, has been completed in approximately 10 h, and the dashed curve shows that, when tension control alone is employed, the tether becomes slack at a length of 5.2 km.

The case for thrust augmentation is made most convincingly in Fig. 3, showing the out-of-plane response. With tension control alone, the angle builds up catastrophically, whereas motion is subdued when tension control is augmented by firing out-of-plane thrusters when the absolute value of the out-of-plane angle first reaches the value of 0.35 rad, and continuing to fire thereafter. (A discussion for the choice of this threshold value of 0.35 rad is given in Sec. III.)

Figure 4, displaying in-plane-angle behavior, also shows the advantage of thrust augmented tension control over tension control alone. It is noteworthy that in the present instance the in-plane thrusters are fired solely near the end of the retrieval, when the satellite is reeled in rapidly. Nevertheless, in-plane behavior is kept under control throughout the entire retrieval due to the coupling of the in-plane motion with the controlled out-of-plane motion.

Time histories for out-of-plane and in-plane thrust are shown by the solid and dashed curves, respectively, in Fig. 5. A thrust limit of 5 N is arbitrarily set to reflect hardware limitations. The thruster saturation indicated in Fig. 5, and later in Fig. 9, is associated solely with the large initial angles used in the simulations and is *not* inherent in the nonlinear thruster control law presented in Sec. III. The total thrust impulse required, including that required for tension augmentation, is 35,300 N-s for a 450-kg satellite.

The principal objectives in using thrust-augmented control are to prevent tether slackness and to stabilize in-plane and out-of-plane motions. An important secondary objective is to speed up the retrieval process, which becomes possible because of the stabilizing action of the thrusters. To illustrate this, we work with the same thrust control law underlying Figs. 1-5, but specify, in the tension control law, a higher rate of retrieval than that used previously. The results are presented in Figs. 6-9.

Figure 6 shows the tether length, in-plane angle, and out-of-plane angle as functions of time. In this instance, both in-plane and out-of-plane thrusters are fired nearly simultaneously, with the in-plane thruster being switched on when the in-plane angle first becomes less than -0.35 rad,

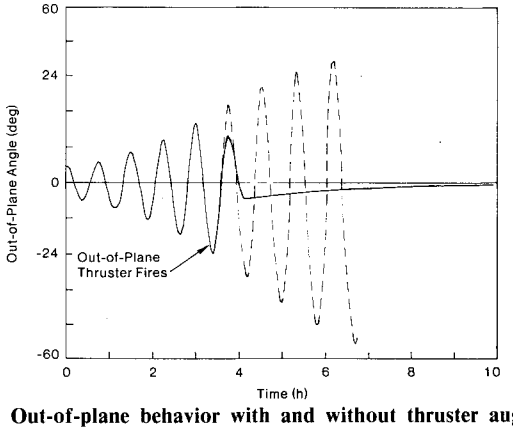

Fig. 3 Out-of-plane behavior with and without thruster augmentation.

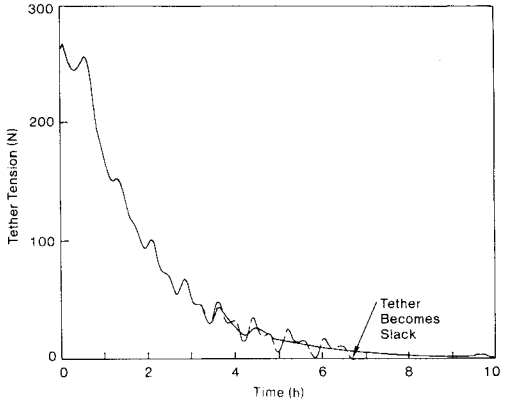

Fig. 1 Tether tension with and without thruster augmentation.

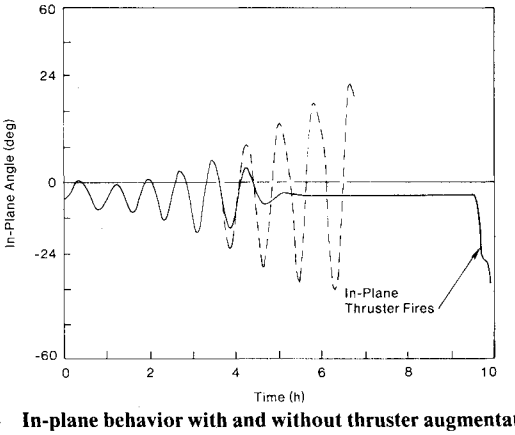

Fig. 4 In-plane behavior with and without thruster augmentation.

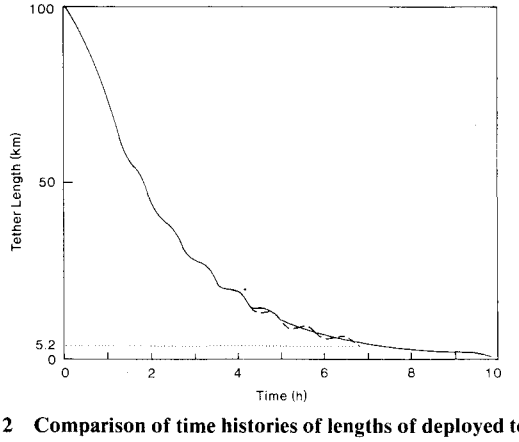

Fig. 2 Comparison of time histories of lengths of deployed tether.

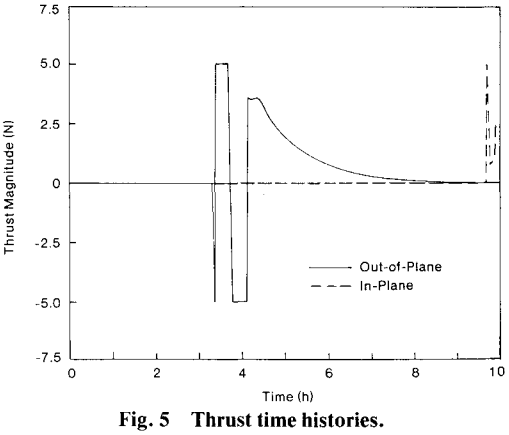

Fig. 5 Thrust time histories.

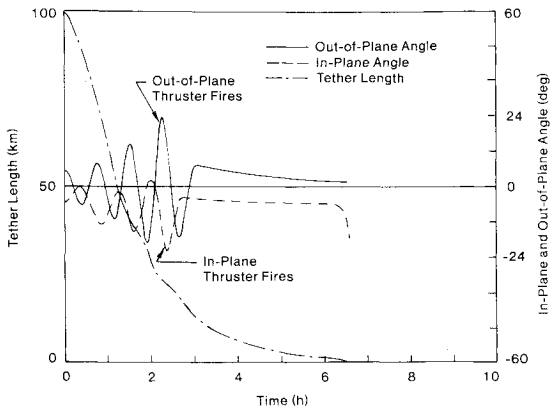

Fig. 6 Fast retrieval with thruster augmented tension control.

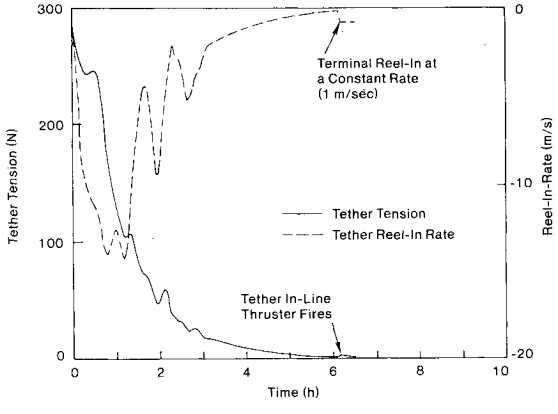

Fig. 7 Tether tension and retrieval rate for fast retrieval.

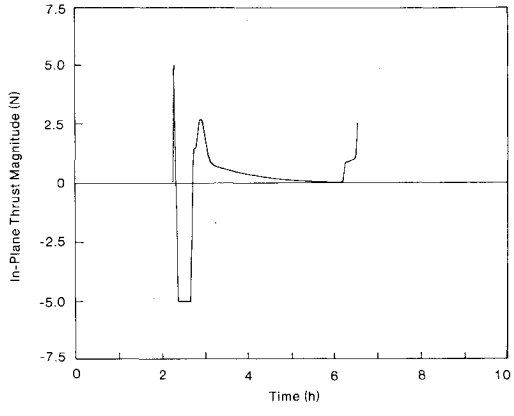

Fig. 8 In-plane thrust for fast retrieval.

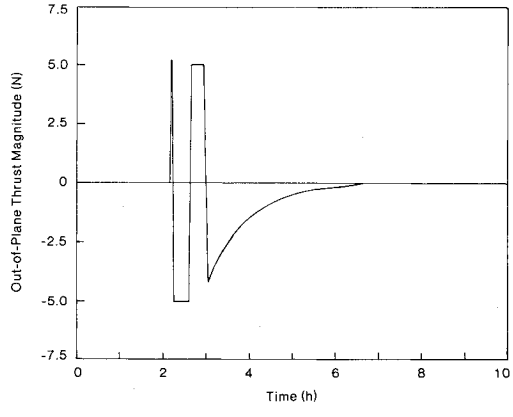

Fig. 9 Out-of-plane thrust for fast retrieval.

and the out-of-plane thruster switched on when the absolute value of the out-of-plane angle first reaches 0.35 rad.

Figure 7 contains the time histories of the tether reel-in rate and the tether tension. Here it can be seen that, when the tension receives a boost due to thruster firing, the satellite is reeled in at a rate of 1 m/s. Normally, in the absence of side thrust, stable retrieval is possible only at a very low rate at this stage of the retrieval process, and it thus takes an inordinately long time to bring the satellite close to the Orbiter. A high terminal retrieval rate, such as 1 m/s, cuts down overall retrieval time and is made possible by using the in-plane thruster to prevent a wrapup.

In-plane and out-of-plane thrust time histories are given in Figs. 8 and 9. The associated thrust limits are set at 5 N as before. Comparing Figs. 8 and 9 with Fig. 5, one sees that during the faster retrieval both the in-plane and out-of-plane thrusters are called on for longer duty than during the slower retrieval. The total thrust impulse required for this case is 45,444 N-s.

When simulations are performed with initial in-plane and out-of-plane angles having smaller values than those considered so far, it is found that the retrieval time for thruster-augmented tension control remains about the same, but there is less angle buildup and less total thrust impulse is required.

III. Theory

Figure 10 is a schematic representation of an Orbiter-mounted, smooth drum D of radius r and axial moment of inertia J, an extensible tether T of mass ρ per unit of length and having a total length L, and a particle satellite S of mass m. The Orbiter (not shown) is presumed to be Earth-pointing and moving in an Earth-centered polar circular orbit of radius R.

To describe the orientation of T, we first introduce a dextral set of mutually perpendicular unit vectors $\boldsymbol{a}_1$, $\boldsymbol{a}_2$, $\boldsymbol{a}_3$,

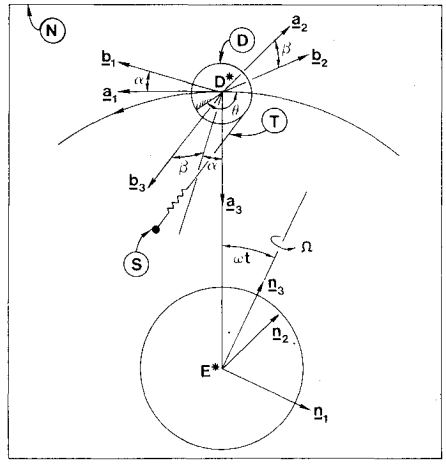

Fig. 10 Schematic representation of tethered satellite system.

with $\boldsymbol{a}_1$ pointing in the direction of motion of D^*, the center of D, and $\boldsymbol{a}_3$ pointing from D^* toward E^*, the center of the Earth. Next, we let $\boldsymbol{b}_1$, $\boldsymbol{b}_2$, $\boldsymbol{b}_3$ form a similar set of unit vectors, align these with $\boldsymbol{a}_1$, $\boldsymbol{a}_2$, $\boldsymbol{a}_3$, respectively, and then subject them successively to a rotation of amount α about a line parallel to $\boldsymbol{a}_2$, and a rotation of amount β about a line parallel to $\boldsymbol{b}_1$. Finally, we take T to be parallel to $\boldsymbol{b}_3$. Thus α and β measure the so-called in-plane and out-of-plane tether angle, respectively.

Drum rotations are characterized by the angle θ between a line parallel to $\boldsymbol{a}_1$ and a line fixed in D. The line joining D^* to E^* is presumed to move in a Newtonian reference frame N, with a constant angular speed ω. This is equivalent to assuming that the center of mass of the Shuttle-tether-satellite

system moves in a circular orbit. Letting $\boldsymbol{n}_1$, $\boldsymbol{n}_2$, $\boldsymbol{n}_3$ be mutually perpendicular unit vectors fixed in N, with $\boldsymbol{n}_3$ parallel to Earth's polar axis, we can thus set the angle between the polar axis and line E^*D^* equal to ωt. Finally, the angular speed of Earth in N is denoted by Ω, a quantity needed for the evaluation of aerodynamic drag forces.

Letting ν be the number of extensional tether vibration modes to be taken into account, and denoting the associated modal coordinates by $q_1,\ldots,q_\nu$, one can introduce $\nu+3$ generalized speeds[11] as

$$u_1 \triangleq r\dot{\theta} \tag{1}$$

$$u_{1+i} \triangleq \dot{q}_i \quad (i=1,\ldots,\nu) \tag{2}$$

$$u_{\nu+2} \triangleq \dot{\alpha} \tag{3}$$

$$u_{\nu+3} \triangleq \dot{\beta} \tag{4}$$

and $\nu+3$ differential equations then can be formulated by using Kane's dynamical equations (Ref. 11, p. 273), considering contributions to the generalized active forces from gravity, rotating Earth aerodynamics, tether elasticity, control torque action on the tether drum D, and thruster action on satellite S. The key steps in the derivation of the equations follow.

The generalized inertia force, F_i^* corresponding to the ith generalized speed is given by

$$F_i^* = -\left[\boldsymbol{\omega}_i^D \cdot (J\boldsymbol{\alpha}^D) + \int_0^{L/r} \boldsymbol{v}_i^{P'} \cdot \boldsymbol{a}^{P'} \rho r \mathrm{d}\psi + \int_{L-r\theta}^{L} \boldsymbol{v}_i^P \cdot \boldsymbol{a}^P \rho \mathrm{d}x + \boldsymbol{v}_i^S \cdot (m\boldsymbol{a}^S)\right] \quad (i=1,\ldots,\nu+3) \tag{5}$$

where $\boldsymbol{\omega}_i^D$, $\boldsymbol{v}_i^{P'}$, $\boldsymbol{v}_i^P$, $\boldsymbol{v}_i^S$ are the ith partial angular velocity (11) of D, partial velocity (11) of a particle P' of the tether on D, partial velocity of a particle P on the deployed part of the tether, and partial velocity of particle S, respectively. Quantities $\boldsymbol{\alpha}^D$, $\boldsymbol{a}^{P'}$, $\boldsymbol{a}^P$, $\boldsymbol{q}^S$ are, respectively, the angular acceleration of D, and the acclerations of P', P, and S. The required partial velocities and accelerations are all derivable (11) from the corresponding velocity expressions. The angular velocity of the drum D is

$$\boldsymbol{\omega}^D = (u_1/r - \omega)\boldsymbol{a}_2 \tag{6}$$

The velocity of the point P' for which the tether wrap angle is ψ and the tangent vector $\boldsymbol{\tau}^{P'}$ is

$$\boldsymbol{v}_i^{P'} = \omega R\boldsymbol{a}_1 + \left(\frac{u_1}{r} - \omega\right) r\boldsymbol{\tau}^{P'} + \sum_{i=1}^{\nu} \phi_i \left[\frac{(\psi-\theta)r}{L}\right] u_{1+i}\boldsymbol{\tau}^{P'} \tag{7}$$

The velocity of the particle P which, when T is unstretched, is at a distance x from the point at which T is attached to D is

$$\boldsymbol{v}^P = \omega R\boldsymbol{a}_1 + [(u_{\nu+2} - \omega)\boldsymbol{a}_2 + u_{\nu+3}\boldsymbol{b}_1] \times (y\boldsymbol{b}_3) + \left[u_1 + \sum_{i=1}^{\nu} \phi_i\left(\frac{x}{L}\right) u_{1+i}\right]\boldsymbol{b}_3 \tag{8}$$

where

$$y = x + \sum_{i=1}^{\nu} \phi_i\left(\frac{x}{L}\right) q_i(t) - (L - r\theta) \tag{9}$$

$\boldsymbol{v}^S$ is obtained from $\boldsymbol{v}^P$ by setting $x=L$ in Eq. (8).

The generalized active force F_i', reflecting the control torque $T_c\boldsymbol{a}_2$ on D, the gravitational forces acting on the tether and satellite, and the thrust F on the satellite, is given by

$$F_i' = \boldsymbol{\omega}_i^D \cdot (T_c\boldsymbol{a}_2) + \int_\theta^{L/r} \boldsymbol{v}_i^{P'} \cdot (\rho g_o \boldsymbol{a}_3) r \mathrm{d}\psi + \int_{L-r\theta}^{L} \boldsymbol{v}_i^P \cdot \boldsymbol{f}_g(x)\mathrm{d}x + \boldsymbol{v}_i^S \cdot [m\boldsymbol{f}_g(L) + F] \quad (i=1,\ldots,\nu+3) \tag{10}$$

where

$$\boldsymbol{f}_g(x) = \rho g_o [\{1 + 3(y/R)\cos\alpha\cos\beta\}\boldsymbol{a}_3 - (y/R)\boldsymbol{b}_3] \tag{11}$$

and g_o is the acceleration due to Earth's gravity at the orbit. The contribution to the generalized forces associated with rotating Earth aerodynamics is given by

$$F_i'' = -\tfrac{1}{2}C_d f \int_{L-r\theta}^{L} \boldsymbol{v}_i^P \cdot \boldsymbol{v}_w \rho_T \mathrm{d}x - \tfrac{1}{2}C_D \rho_s A_S \boldsymbol{v}_i^S \cdot |\boldsymbol{v}_w| \boldsymbol{v}_w \quad (i=1,\ldots,\nu+3) \tag{12}$$

where

$$\boldsymbol{v}_w = \omega R\boldsymbol{a}_1 + \Omega R \sin\omega t \boldsymbol{a}_2 \tag{13}$$

and the notations $C_d, f, \rho_T, C_D, \rho_S, A_S$ are explained later.

The generalized force contribution associated with tether longitudinal viscoelasticity, evaluated as shown in Ref. 10, is given by

$$F_i''' = -A_T \sum_{i=1}^{\nu} (Eq_i + Fu_{1+i}) \left\langle \int_{L-r\theta}^{L} \frac{\mathrm{d}}{\mathrm{d}x}\left[\phi_i\left(\frac{x}{L}\right)\right] \times \frac{\mathrm{d}}{\mathrm{d}x}\left(\boldsymbol{v}_i^P \cdot \boldsymbol{b}_3\right)\mathrm{d}x + \frac{1}{r}\int_\theta^{L/r} \frac{\mathrm{d}}{\mathrm{d}\psi}\left[\phi_i\left\{(\psi-\theta)\frac{r}{L}\right\}\right] \times \frac{\mathrm{d}}{\mathrm{d}\psi}\left(\boldsymbol{v}_i^{P'} \cdot \boldsymbol{\tau}^{P'}\right)\mathrm{d}\psi\right\rangle \quad (i=1,\ldots,\nu+3) \tag{14}$$

Substituting from Eq. (5) and Eqs. (10-14) into Kane's equations written as

$$-F_i^* = F_i' + F_i'' + F_i''' \quad (i=1,\ldots,\nu+3) \tag{15}$$

one arrives at

$$\left(m + \rho L + \frac{J}{r^2}\right)\dot{u}_1 + \sum_{i=1}^{\nu}\left[m\sin\gamma_i + \frac{\rho L}{\gamma_i}(1-\cos\gamma_i)\right]\dot{u}_{1+i} = I_1\left[u_{\nu+3}^2 + (u_{\nu+2}-\omega)^2\cos^2\beta + \omega^2(3\cos^2\alpha\cos^2\beta - 1)\right] - \tfrac{1}{2}(\omega R\sin\alpha\cos\beta - \Omega R\sin\beta\sin\omega t) \times \left[fc_d\int_{L-r\theta}^{L}\rho_T\mathrm{d}x + h\right] + \frac{T_C}{r} \tag{16}$$

$$\dot{u}_1\left[m\sin\gamma_i + \frac{\rho L}{\gamma_i}(1-\cos\gamma_i)\right] + \sum_{j=1}^{\nu}\dot{u}_{1+j}\left\{m\sin\gamma_i\sin\gamma_j + \frac{\rho L}{2}\left[\frac{\sin(\gamma_i-\gamma_j)}{\gamma_i-\gamma_j} - \frac{\sin(\gamma_i+\gamma_j)}{\gamma_i+\gamma_j}\right]\right\} = I_{3+i}\left[u_{\nu+3}^2 + (u_{\nu+2}-\omega)^2\cos^2\beta + \omega^2(3\cos^2\alpha\cos^2\beta - 1)\right] - \tfrac{1}{2}(\omega R\sin\alpha\cos\beta - \Omega R\sin\beta\sin\omega t) \times \left[fc_d\int_{L-r\theta}^{L}\rho_T\varphi_i\left(\frac{x}{L}\right)\mathrm{d}x + h\varphi_i(1)\right] - A\sum_{j=1}^{\nu}(Eq_j + Fu_{1+j})\frac{\gamma_i\gamma_j}{2L}\left[\frac{\sin(\gamma_i-\gamma_j)}{\gamma_i-\gamma_j} + \frac{\sin(\gamma_i+\gamma_j)}{\gamma_i+\gamma_j}\right] + \tau\varphi_i(1) \quad (i=1,\ldots,\nu) \tag{17}$$

$$\dot{u}_{\nu+2}=2(u_{\nu+2}-\omega)u_{\nu+3}\tan\beta-3\omega^2\sin\alpha\cos\alpha$$
$$-2\frac{I_3}{I_2}(u_{\nu+2}-\omega)-\frac{\omega R\cos\alpha}{2I_2\cos\beta}\left\{fc_d\int_{L-r\theta}^{L}\rho_T\left[x+\sum_{i=1}^{\nu}\varphi_i\left(\frac{x}{L}\right)q_i-L+r\theta\right]dx+h\left[r\theta+\sum_{i=1}^{\nu}\varphi_i(1)q_i\right]\right\}+F_\alpha \tag{18}$$

$$\dot{u}_{\nu+3}=-\left[(u_{\nu+2}-\omega)^2+3\omega^2\cos^2\alpha\right]\sin\beta\cos\beta$$
$$-2\frac{I_3}{I_2}u_{\nu+3}+\frac{\omega R\sin\alpha\sin\beta+\Omega R\sin\omega t\cos\beta}{2I_2}$$
$$\times\left\{fc_d\int_{L-r\theta}^{L}\rho_T\left[x+\sum_{i=1}^{\nu}\varphi_i\left(\frac{x}{L}\right)q_i-L+r\theta\right]dx+h\left[r\theta+\sum\varphi_i(1)q_i\right]\right\}+F_\beta \tag{19}$$

where $I_1,\ldots,I_{3+i}$ $(i=1,\ldots,\nu)$, f, and h are defined as

$$I_1\triangleq\int_{L-r\theta}^{L}\rho\left[x+\sum_{i=1}^{\nu}\varphi_i\left(\frac{x}{L}\right)q_i-L+r\theta\right]dx+m\left[r\theta+\sum_{i=1}^{\nu}\varphi_i(1)q_i\right] \tag{20}$$

$$I_2\triangleq\int_{L-r\theta}^{L}\rho\left[x+\sum_{i=1}^{\nu}\varphi_i\left(\frac{x}{L}\right)q_i-L+r\theta\right]^2dx+m\left[r\theta+\sum_{i=1}^{\nu}\varphi_i(1)q_i\right]^2 \tag{21}$$

$$I_3\triangleq\int_{L-r\theta}^{L}\rho\left[x+\sum_{i=1}^{\nu}\varphi_i\left(\frac{x}{L}\right)q_i-L+r\theta\right]\times\left[u_1+\sum_{j=1}^{\nu}\varphi_j\left(\frac{x}{L}\right)u_{1+j}\right]dx+m\left[r\theta+\sum_{i=1}^{\nu}\varphi_i(1)q_i\right]\left[u_1+\sum_{j=1}^{\nu}\varphi_j(1)u_{1+j}\right] \tag{22}$$

$$I_{3+i}\triangleq\int_{L-r\theta}^{L}\rho\left[x+\sum_{j=1}^{\nu}\varphi_j\left(\frac{x}{L}\right)q_j-L+r\theta\right]\varphi_i\left(\frac{x}{L}\right)dx+m\left[r\theta+\sum\varphi_j(1)q_j\right]\varphi_i(1)\qquad(i=1,\ldots,\nu) \tag{23}$$

$$f\triangleq\left\{\frac{4A_T}{\pi}\left[\omega^2R^2(1-\sin^2\alpha\cos^2\beta)+\Omega^2R^2\cos^2\beta\sin^2\omega t+2\omega\Omega R^2\sin\alpha\sin\beta\cos\beta\sin\omega t\right]\right\}^{1/2} \tag{24}$$

$$h\triangleq c_D\rho_sA_s\left[\omega^2R^2+\Omega^2R^2\sin^2\omega t\right]^{1/2} \tag{25}$$

and, as in Ref. 10, the extensional vibration modes of T are described in terms of modal functions $\theta_i(x/L)$ given by

$$\varphi_i(x/L)=\sin(\gamma_ix/L)\qquad(i=1,\ldots,\nu) \tag{26}$$

and γ_i satisfies the characteristic equation

$$\gamma_iL-\tan\gamma_iL=\rho L/m\qquad(i=1,\ldots,\nu) \tag{27}$$

Equations (25) and (26) imply that the entire tether is elastic. As has been shown in Ref. 10, this approach leads to the same tension value at the Shuttle end from both modal displacement and modal acceleration points of view. (Models that treat only the deployed portion of the tether as elastic lead to an apparent anomaly in this regard.)

In Eq. (17), E and F are, respectively, coefficients of elasticity and viscoelasticity; aerodynamic drag has been taken into account by employing the same atmospheric density model as in Ref. 2, with c_d, A_T, and ρ_T standing for tether drag coefficient, tether cross-section area, and air density at a point of T, respectively; while c_d, A_s, and ρ_s are corresponding quantities for S. Finally, T_c denotes the control torque applied to D; F_α and F_β are associated, respectively, with the generalized forces due to in-plane and out-of-plane control thrusts applied to S; τ is the tether-aligned thrust, which is equal to zero so long as the tether tension exceeds a specified value (2 N), and is constant otherwise.

A satisfactory torque control law is constructed by building on the work of earlier investigators (Refs. 1, 5-7, 9). No previously published control law involving tension control alone was found adequate to prevent tether slackness entirely. However, the following torque (tension) control law, which has the form proposed by Modi et al.,[9] produces good results when used in conjuction with thruster control:

$$\frac{T_c}{r}=-3\left(m+\frac{\rho r\theta}{2}\right)\omega^2r\theta+\left(m+\rho L+\frac{J}{r^2}\right)\{4\omega^2(\ell_c-r\theta)-4\omega u_1-\ell_c[\omega u_{\nu+2}+\omega u_{\nu+3}+\omega^2\alpha+\omega^2\beta]\} \tag{28}$$

with

$$\ell_c=\ell_o\exp(-\epsilon t) \tag{29}$$

where ℓ_o is the inially deployed length of the tether, and ϵ is the retrieval rate control parameter, with $\epsilon=1.27$ for Figs. 1-5, and $\epsilon=2.00$ for Figs. 6-9. As for thrust control, this is specified such that the in-plane thruster, associated with the term F_α in Eq. (18), begins firing when α first attains the value of -0.35 rad, and continues to fire thereafter (regardless of the value of α); the out-of-plane thruster, associated with F_β in Eq. (10), is first fired when $|\beta|>0.35$ rad, and continues to fire thereafter. A threshold value is set for the angles to reduce the burden on the thrusters; that is, the thrusters go into action only after the tension control operation has removed some of the energy in the system. This conserves fuel consumption. However, delaying the thruster firing too long can be fatal, making it impossible to achieve stable operation. The threshold value of ±0.35 rad represents a suitable compromise, as revealed by numerous simulations. Expressions for F_α and F_β, representing thrust control action in Eqs. (18) and (19), respectively, are chosen to be

$$F_\alpha=2(\delta-\zeta\omega\sqrt{3})u_{\nu+2} \tag{30}$$

$$F_\beta=2(\delta-2\zeta\omega)u_{\nu+3} \tag{31}$$

with $\zeta=10.0$, and

$$\delta=\left(m+\frac{\rho r\theta}{2}\right)r\theta u_1\Big/\left\{mr^2\theta^2+\frac{\rho L}{3}L^2\left[1-\left(1-\frac{r\theta}{L}\right)^3\right]-\rho r\theta L^2\left(1-\frac{r\theta}{L}\right)\right\} \tag{32}$$

Equations (30) and (31) correspond to a physical side thrust F given by

$$F=F_1b_1+F_2b_2 \tag{33}$$

with

$$F_1 = F_\alpha I_2 \cos\beta / r\theta \tag{34}$$

$$F_2 = -F_\beta I_2 / r\theta \tag{35}$$

The rationale underlying this choice of functional forms is to attempt to annul in the equations of motion terms normally associated with "negative damping."

Finally, the key control step for the last stage of retrieval is to start the tether-aligned thruster of thrust magnitude 2 N when the natural tether tension first goes below this value, and then to maintain this constant thrust of 2 N for the rest of the retrieval. (The thrust level of 2 N is chosen because hardware tests reveal that this same level of thrust is needed during initial deployment of the satellite merely to overcome the friction in the tether-pully system.) With tether tension maintained in this way, the final strategy is then to reel in the satellite at a high rate, such as the rate of 1 m/s used in these simulations, while relying on the in-plane thruster to prevent tether wrap-up.

IV. Conclusion

The simulation results reported in Sec. II justify the conclusion that thrust augmentation of tension and the use of transverse thrust are needed to maintain control and expedite the retrieval process. These measures necessarily increase both the mass of the satellite (by about 40%) and satellite power requirements, but these are small prices to pay for the positive control action and the reduction in retrieval time.

In the analytical model used in this paper, we have accounted for tether extensibility, gravity, and rotating Earth aerodynamics, but have neglected to account for friction between the tether and the drum, flexure of the tether, rigid-body effects of the satellite, and the pulsed nature of the thrust that has to replace the continuous level of thrust assumed in our analysis. Consideration of these effects will doubtlessly modify some of the results presented here, but we believe that the main conclusion established in this paper, namely, the necessity and the benefit of using thrusters to augment tension control, will not change.

V. Acknowledgment

Acknowledgment is made to our former association with Martin-Marietta Aerospace, Denver, Colo., where the idea of thrust augmented control was developed.

References

[1] Baker, W.P., Dunkin, J.A., Galaboff, A.J., Johnston, K.D., Kissel, R.R., Rheinfurth, M.H., and Siebel, M.P.P., "Tethered Subsatellite Study," NASA TM X-73314, March 1976.

[2] Kallaghan, P.N., Arnold, D.A., Colombo, G., Grossi, M.D., Kirschner, L.R., and Orringer, O., "Study of the Dynamics of a Tethered Satellite System (Skyhook)," Smithsonian Astrophysical Observatory, Cambridge, Mass., Final Report, 1978.

[3] Misra, A.K. and Modi, V.J. "A General Dynamical Model for the Space Shuttle Based Tethered Subsatellite System," *Advances in the Astronautical Sciences,* Vol. 40, Part II, 1979, pp. 537-557.

[4] Weber, R. and Brauchli, H., "Dynamics of a System of Two Satellites Connected by a Deployable and Extensible Tether of Finite Mass," Vols. I and II, ETH, Zurich, Swiss Federal Institute of Technology Report, ESTEC Contract No. 2992/76/NL/AK(SC), 1978.

[5] Rupp, C.C., "A Tether Tension Control Law for Tethered Satellites Deployed Along the Local Vertical," NASA TM X-64963, 1975.

[6] Kulla, P., "Stabilization of Tethered Satellites," European Space Agency Report, TMM/78-07/PK-avs, 1977.

[7] Bainum, P.M. and Kumar, V.K., "Optimal Control of the Shuttle-Tethered-Subsatellite System," *Acta Astronautica,* Vol. 7, No. 12, 1980, pp. 1333-1348.

[8] Misra, A.K. and Modi, V.J., "Deployment and Retrieval of a Subsatellite Connected by a Tether to the Space Shuttle," *Journal of Guidance, Control, and Dynamics,* Vol. 5, May 1982, pp. 278-285.

[9] Modi, V.J., Geng, Chang-fu, and Misra, A.K., "Effect of Damping on the Control Dynamics of the Space Shuttle Based Tethered System," AAS/AIAA Paper 81-143, Lake Tahoe, Nev., Aug. 3-5, 1981.

[10] Banerjee, A.K. and Kane, T.R., "Tether Deployment Dynamics," *Journal of the Astronautical Sciences,* Vol. XXX, Oct.-Dec. 1982, pp. 347-366.

[11] Kane, T.R., Likins, P.W., and Levinson, D.A., *Spacecraft Dynamics,* McGraw-Hill, New York, 1982, p. 87.